

# Joint Synchronization and Equalization in the Uplink of Multi-user OPRFB Transceivers

Siavash Rahimi and Benoit Champagne

Department of Electrical and Computer Engineering, McGill University

3480 University St., Montreal, Quebec, Canada, H3A 0E9

**Abstract**—This paper addresses the problem of carrier frequency synchronization and time-varying channel equalization in the uplink of a broadband multi-user wireless communication system employing an oversampled perfect reconstruction filter bank (OPRFB) transceiver structure for multi-carrier modulation. Based on the maximum likelihood (ML) principle, a pilot-aided joint estimator of the carrier frequency offsets (CFO) and channel equalizer coefficients of the multiple users is proposed. The performance of the new estimator is examined for various subband allocation schemes by means of numerical simulations under realistic conditions of operation. For mobile users with time-varying fading channels, we also study the effect of using different distributions of pilots over time. Our results show that the proposed estimator can provide accurate estimates of the unknown CFO and channel parameters, which in turn can be used to design effective compensation mechanisms.

**Index Terms**—Multi-user, data-aided estimation, synchronization, equalization, filter bank transceiver.

## I. INTRODUCTION

In recent years, a multi-user extension of orthogonal frequency division multiplexing (OFDM) known as orthogonal frequency division multiple access (OFDMA) has become part of the new standards for broadband wireless access [1]. Despite its appealing features, OFDMA imposes strict requirements on the frequency synchronization, where inaccurate compensation of carrier frequency offset (CFO) results in intercarrier interference (ICI) and multiple access interference (MAI), while timing error leads to interblock interference (IBI). These interference sources may severely degrade the link quality, resulting in unacceptable error rates [2].

Filter bank multicarrier (FBMC) systems [3] have been proposed as an alternative to OFDM due to the high spectral containment of their subband filters that effectively cancel MAI [4]. It has been shown that in a multi-user context, FBMC techniques can achieve lower error rates with reduced computational complexity in interference cancellation compared to OFDMA [4], [5]. Also, most of the FBMC methods allow unsynchronized users to transmit simultaneously, which dramatically increases the system flexibility. Among the various approaches available for the design of FBMC transceiver systems, lately, much interest has been directed towards oversampled perfect reconstruction filter banks (OPRFB), e.g. [6], [7]. Indeed, OPRFB benefits from improved robustness against narrowband interference and CFO, while its multi-user implementation (i.e., MU-OPRFB) is straightforward. In contrast to OFDM and some other FBMC methods that require at least one empty frequency subband between contiguous

groups of sub-carriers allocated to different users, MU-OPRFB systems can still separate the users without employing such guard bands due to the high selectivity of their subband filters and consequently, higher spectral efficiency can be achieved. Albeit to a lesser extent than OFDM and other FBMC systems, OPRFB transceivers remain sensitive to CFO, which will lead to a performance degradation unless it is properly compensated. Also, the deleterious effect of frequency selective channels in these transceivers should be removed through equalization. In the case of mildly selective channels with a large number of narrow subbands, it is sufficient to use single-tap per subband equalizers for OPRFB systems [6], whereas for highly selective channels, more advanced equalization techniques may be required.

The estimation procedure of CFO and channel equalizer coefficients in the downlink of MU-OPRFB systems is similar to the single-user OPRFB situation. That is, each mobile terminal (MT) exploits a dedicated subset of received pilot symbols to find the unknown parameters for its particular connection as in [8]. However, this process in the uplink is more challenging, since the signal received by the base station (BS) results from the superposition of the individual users' transmitted signals, each one affected by a different CFO and channel impulse response (CIR). Once the uplink CFO and CIR coefficients of each user have been estimated, they must be employed to compensate the associated impairments through appropriate frequency synchronization and channel equalization mechanisms. Several methods have been proposed for CFO compensation in FBMC systems [9], [10], however, they are not suitable for OPRFB transceivers due to inherent structural differences (especially, the use of longer prototype filters). Recently, a maximum likelihood (ML) estimator of the CFO and CIR for application in *single-user* OPRFB transceiver system has been investigated in [11]. Still, this method is not directly suitable to address the synchronization and channel equalization requirements in multi-user systems.

In this paper, we develop a data-aided joint maximum likelihood (ML) estimator of the CFO and CIR that is specifically designed for the uplink of MU-OPRFB systems operating over frequency selective fading channels. The estimated CFO and CIR parameters are used to design effective compensation mechanisms for each individual user, i.e., frequency synchronization and single-tap per subband equalizer. The performance of the proposed synchronization and equalization methods is investigated via computer simulations for various subband allocation schemes with different pilot distributions over time-invariant and time-varying (mobile) channels.

The paper is organized as follows. Section II presents the

This work was supported by the Natural Sciences and Engineering Research Council of Canada (NSERC). Email: benoit.champagne@mcgill.ca

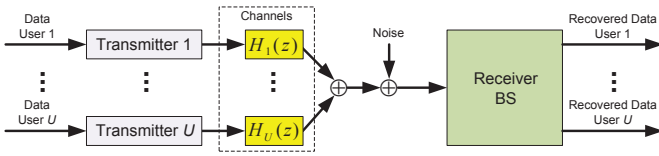


Fig. 1. Uplink transmissions in MU-OPRFB system

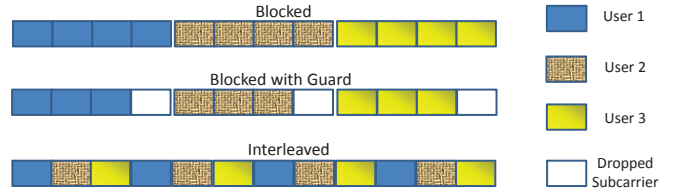
MU-OPRFB system model. The joint ML estimator of the CFO and equalizer coefficients is developed in Section III. The performance of the proposed joint estimator is evaluated in Section IV and some conclusions are offered in Section V.

## II. MULTI-USER OPRFB SYSTEM MODEL

We consider uplink transmissions in a MU-OPRFB system, as depicted in Fig. 1, where  $U$  denotes the number of users. A total of  $M$  subbands, indexed from 0 to  $M-1$  and shared among the  $U$  users, are available for multicarrier transmission. The set of subbands allocated to user  $u \in \{1, \dots, U\}$  is represented as  $\mathcal{S}_u = \{\varsigma_1^u, \dots, \varsigma_{|\mathcal{S}_u|}^u\}$ , where  $0 \leq \varsigma_1^u < \dots < \varsigma_{|\mathcal{S}_u|}^u \leq M-1$  and  $|\mathcal{S}_u|$  denotes the cardinal number of set  $\mathcal{S}_u$ . Note that no subband is shared between different users, i.e.,  $\mathcal{S}_u \cap \mathcal{S}_v = \emptyset$ , for  $u \neq v$ . Three frequency subband allocation schemes, namely blocked, blocked with guard and interleaved, are considered in this work, as depicted in Fig. 2. The blocked scheme allocates a contiguous group of subbands to each user, whereas in blocked with guard scheme, one subband is left unused between the blocks of subbands assigned to different users. Alternatively, to exploit the frequency diversity of multipath channels, the interleaved scheme is considered where each user's allocated subbands are uniformly spaced over the channel bandwidth. Although the available subbands are evenly divided between users in this work, the above schemes can easily be expanded to uneven allocations to meet specific QoS requirements in a given application.

As shown in [2], the proper choice of CFO estimation method in the multi-user context depends on the adopted subband allocation scheme. Moreover, channel estimation can only be performed within the allocated subbands of each individual user separately, as each user is only assigned a subset of the whole frequency band. Recently, the block allocation has drawn more attention from standard bodies, as in e.g. LTE release 8 [1] where users can select the best available blocks based on signal-to-noise ratio (SNR) indicators. Hence, it is of special interest to develop synchronization and equalization methods that perform well with common allocation schemes and, in particular, with the blocked scheme.

The MU-OPRFB transceiver for the  $u$ th user is depicted in block diagram form in Fig. 3, where  $K$  represents the upsampling/downsampling factor and  $K > M$  is assumed (oversampling) [6]. For  $i \in \{1, \dots, |\mathcal{S}_u|\}$ ,  $x_i^u[n]$  denotes the complex-valued symbol sequence transmitted by this user on the  $i$ th subband of the set  $\mathcal{S}_u$  at discrete-time  $nT_s$ , where  $n \in \mathbb{Z}$ ,  $T_s = F_s^{-1}$  and  $F_s$  is the input sampling rate. In MU-OPRFB systems, the transmit and receive subband filters are derived from common prototypes with finite impulse responses (FIR) of length  $D$  and respective system functions  $F_0(z) = \sum_{n=0}^{D-1} f_0[n]z^{-n}$  and  $G_0(z) = \sum_{n=0}^{D-1} g_0[n]z^{-n}$ .


 Fig. 2. Allocation schemes with  $U = 3$  users over  $M = 12$  subbands

For convenience in analysis,  $G_0(z)$  is assumed non-causal although in practice, causality can be restored simply by introducing an appropriate delay in the receiver. Defining  $w = e^{-j2\pi/M}$ , the DFT modulated transmit and receive filters for the  $i$ th subband of the  $u$ th user are respectively obtained as  $F_i^u(z) = F_0(zw^{\varsigma_i^u})$  and  $G_i^u(z) = G_0(zw^{\varsigma_i^u})$ . As proposed in [6], to enforce the perfect reconstruction (PR) property, the paraconjugates of the transmit filters are employed as receive filters, i.e.,  $g_i^u[n] = f_i^u[n]^*$ . In this work, the filter length  $D$  is restricted to be a multiple of  $M$  and  $K$ , i.e.,  $D = d_P P$ , where  $P$  denotes the least common multiple of  $M$  and  $K$  and  $d_P$  is an integer. The transmitter output signal of the  $u$ th user at discrete-time  $mT_s/K$ , is given by

$$y_u[m] = \sum_{i \in \mathcal{S}_u} \sum_q x_i^u[q] f_i^u[m - qK] \quad (1)$$

where the range of the summation over  $q$  is delimited by the finite support of the subband FIR filters,  $f_i^u[m]$ .

We assume that during a time interval equal to the processing delay of the transceiver system (i.e.,  $2DT_s/K$ ), the transmission channel of the  $u$ th user can be modeled as a linear time-invariant system with FIR  $h_u[l]$  of length  $Q$  and corresponding system function,  $H_u(z) = \sum_{l=0}^{Q-1} h_u[l]z^{-l}$ . Similar to OFDMA, MU-OPRFB systems are mostly tailored to provide wireless connectivity to devices with low mobility, and therefore the channel coherence time is much larger than the symbol duration. Consequently, we can assume that the channel remains static over several MU-OPRFB symbols. In the presence of CFO, the received signal from the  $u$ th user, can be modeled as

$$\bar{y}_u[m] = e^{j2\pi \frac{\mu_u}{M} m} \sum_{l=0}^{Q-1} h_u[l] y_u[m-l] \quad (2)$$

where  $\mu_u$  is the normalized CFO with respect to the subband spacing  $F_s K/M$ .

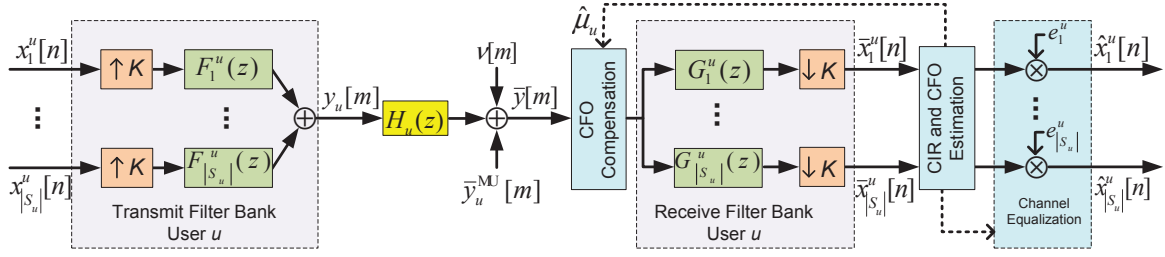
The received signal at the BS is corrupted by an AWGN sequence  $\nu[m]$ , statistically independent from the input data, with zero-mean and variance  $E\{|\nu[m]|^2\} = \sigma_\nu^2$ , where  $E\{\cdot\}$  denotes statistical expectation. The received baseband discrete-time signal  $\bar{y}[m]$  can therefore be expressed as

$$\bar{y}[m] = \bar{y}_u[m] + \bar{y}_u^{\text{MU}}[m] + \nu[m] \quad (3)$$

where  $\bar{y}_u^{\text{MU}}[m]$  represents the transmitted signals from all users other than the  $u$ -th one:

$$\bar{y}_u^{\text{MU}}[m] = \sum_{\substack{v=1 \\ v \neq u}}^U \bar{y}_v[m] \quad (4)$$

On the receiver side, signal  $\bar{y}[m]$  is passed through a bank of analysis filters and downsampled by  $K$ . Accordingly, the


 Fig. 3. Transceiver chain of the  $u$ th user in a MU-OPRFB system with CFO and channel estimation

reconstructed signal for the  $i$ th subband of the  $u$ th user can be written as

$$\begin{aligned} \bar{x}_i^u[n] &= \sum_q \bar{y}[q] f_i^u[q - nK]^* \\ &= \sum_{l=0}^{Q-1} \sum_p \sum_{j \in \mathcal{S}_u} x_j^u[p] \gamma_{i,n}^{j,p}(l, \mu_u, u) h_u[l] + \psi_i^u[n] + \nu_i^u[n] \end{aligned} \quad (5)$$

where  $\gamma_{i,n}^{j,p}(l, \mu_u, u)$ ,  $\psi_i^u[n]$  and  $\nu_i^u[n]$  are defined below:

$$\gamma_{i,n}^{j,p}(l, \mu_u, u) = \sum_q e^{j2\pi \frac{\mu_u}{M} q} f_j^u[q - l - pK] f_i^u[q - nK]^* \quad (6)$$

$$\psi_i^u[n] = \sum_q \bar{y}_u^{\text{MU}}[q] f_i^u[q - nK]^* \quad (7)$$

$$\nu_i^u[n] = \sum_q \nu[q] f_i^u[q - nK]^*. \quad (8)$$

The complex factor  $\gamma_{i,n}^{j,p}(l, \mu_u, u)$  characterizes the interference level of the  $p$ th input sample from the  $j$ th subband of user  $u$  on the  $n$ th output sample of the  $i$ th subband of the same user, in the presence of CFO with magnitude  $\mu_u$  through the  $l$ th path of the channel between this user and the BS. The terms  $\psi_i^u[n]$  and  $\nu_i^u[n]$  represent the total contribution to  $\bar{x}_i^u[n]$  from the other users' input symbols (i.e., MAI) and the additive noise to  $\bar{x}_i^u[n]$ , respectively.

Based on our earlier assumptions on the additive noise  $\nu[q]$  in (3) and the PR properties of the subband filters, it can be shown that the noise term  $\nu_i^u[n]$  in (8) is normally distributed with zero-mean and covariance  $E \{ \nu_i^u[p] \nu_j^u[q]^* \} = \delta_{ij} \delta_{pq} \sigma_\nu^2$ , where  $\delta_{ij}$  denotes the Kronecker delta function. A similar conclusion can be reached for the multi-user interference term  $\psi_i^u[n]$  in (7), if we model the input signals from the interfering users, i.e.  $x_i^v[q]$  for all  $v \neq u$  and  $i \in \mathcal{S}_v$ , as independent zero-mean white data sequences with variance  $\sigma_x^2$ . In this case, it follows from (1), (2), (4) and (7) that the multi-user interference term  $\psi_i^u[n]$  is the sum of a large number of independent random contributions. Therefore, based on the central limit theorem [12], this term can be approximated as a normally distributed random variable with zero-mean. In this work, we further assume that in the subband domain,  $\psi_i^u[n]$  can be modeled as a white noise sequence, i.e. with covariance  $E \{ \psi_i^u[p] \psi_j^u[q]^* \} \simeq \delta_{ij} \delta_{pq} \sigma_\psi^2$  where  $\sigma_\psi^2$  is the corresponding variance. We have been able to verify the validity of this result through numerical simulations. In practice,  $\sigma_\psi^2$  can be obtained based on measurements of interference power.

As seen from Fig. 3, if a suitable estimate of  $\mu_u$  is available, say  $\hat{\mu}_u$ , it can be used to compensate the CFO at the receiver front-end on the allocated subbands of the  $u$ th user and thereby avoid its deleterious effects. Similarly, equalizer coefficients, e.g.,  $e_i^u$  for a single-tap per subcarrier equalizer, can be derived based on estimates of the channel coefficients, say  $\hat{h}_u[l]$  for  $0 \leq l < Q$ , in order to reverse the distortion incurred by the input  $x_i^u[n]$  during their transmission. Our interest in this work, therefore, lies in the development of an efficient, data-aided ML-based approach for the estimation of the CFO parameter  $\mu_u$  and the equalizer coefficients  $e_i^u$  for the  $u$ th user. Considering the requirements of multi-user applications, this estimation approach should be able to determine the parameter of interest of the  $u$ th user independently of the transmission state of the other users.

### III. JOINT ESTIMATION

In this section, we derive a joint estimator of CFO and equalizer coefficients for the  $u$ th user, where  $u \in \{1, \dots, U\}$ . We define a vector symbol as the ordered set of subband inputs, i.e.  $x_i^u[n]$  for all  $i \in \mathcal{S}_u$ , entering the transmit filter bank at time  $n$ . We assume that within a burst of  $N$  consecutive vector symbols, say from time  $n = 0$  to  $N - 1$ , a total of  $T_u$  such vectors with time in  $\mathcal{T}_u = \{t_1, \dots, t_{T_u}\}$  are selected for the transmission of pilots, where  $0 \leq t_1 < t_2 < \dots < t_{T_u} \leq N - 1$ . At any given time  $t \in \mathcal{T}_u$ , all the  $|\mathcal{S}_u|$  allocated subbands to the user  $u$ , with indices  $i \in \mathcal{S}_u$ , are dedicated to the transmission of pilot symbols  $p_i^u[t]$ . We therefore consider a rectangular lattice of  $N_u = T_u |\mathcal{S}_u|$  pilot symbols distributed over the time-frequency plane for the  $u$ -th user. In order to track time-varying channels, various distributions of pilots over time are considered in this work. Specifically, the set  $\mathcal{T}_u$  is chosen such that the  $T_u$  pilot vectors are divided into  $G$  groups evenly distributed throughout a burst, with each group consisting of  $T_u/G$  (integer) consecutive vectors. More precisely, we define

$$t_l = \lfloor lG/T_u \rfloor N/G + (l \bmod (T_u/G)) \quad (9)$$

for  $l \in \{0, \dots, T_u - 1\}$ , where  $\lfloor \cdot \rfloor$  and  $\bmod$  denote the floor and modulo operations, respectively. However, our approach can be applied to other distributions of pilot symbols.

Let  $z_i^u[t]$ ,  $t \in \mathcal{T}_u$ , denote the reconstructed signal corresponding to transmitted pilot  $p_i^u[t]$ . From (5), it follows that

$$z_i^u[t] = \sum_{l=0}^{Q-1} \lambda_{i,t}^u(l, \mu_u) h_u[l] + \nu_i^u[t] \quad (10)$$

where we define

$$\lambda_{i,t}^u(l, \mu_u) = \sum_{p \in \mathcal{T}_u} \sum_{j \in \mathcal{S}_u} p_j \gamma_{i,t}^{j,p}(l, \mu_u, u) \quad (11)$$

$$v_i^u[t] = w_i^u[t] + \psi_i^u[t] + \nu_i^u[t] \quad (12)$$

$$w_i^u[t] = \sum_{l=0}^{Q-1} \sum_{p \notin \mathcal{T}_u} \sum_{j \in \mathcal{S}_u} x_j^u[p] \gamma_{i,t}^{j,p}(l, \mu_u, u) h_u[l] \quad (13)$$

Here, the term  $\lambda_{i,t}^u(l, \mu_u)$  represents the contribution from all the pilot symbols to the output  $z_i^u[t]$ , through the  $l$ th channel path, whereas  $w_i^u[t]$  (13) is the total contribution from the non-pilot (i.e., data carrying) symbols to  $z_i^u[t]$  and can be interpreted as a form of data-interference. For similar reason as in the case of the MAI term  $\psi_i^u[n]$  in (7),  $w_i^u[t]$  can be approximated as an independent, circular complex Gaussian random variable with zero-mean and covariance  $E\{w_i^u[t] w_i^{u'}[t']^*\} \simeq \delta_{ii'} \delta_{tt'} \sigma_w^2$ , where

$$\sigma_w^2 = \sigma_x^2 \sum_{p \notin \mathcal{T}_u} \sum_{j \in \mathcal{S}_u} |\Gamma_{i,t}^{j,p}(\mu_u, u)|^2 \quad (14)$$

and  $\Gamma_{i,t}^{j,p}(\mu_u, u) = \sum_{l=0}^{Q-1} \gamma_{i,t}^{j,p}(l, \mu_u, u) h_u[l]$ . Through simulations, we find that  $\sigma_w^2$  is only weakly dependent on  $i, t$  and  $\mu_u$ ; accordingly, we model this quantity as a constant. As a result,  $v_i^u[t]$  is zero-mean with a variance of  $\sigma_v^2 = \sigma_w^2 + \sigma_\psi^2 + \sigma_\nu^2$ .

For convenience, we let  $\mathbf{h}_u = [h_u[0] \ h_u[1] \ \dots \ h_u[Q-1]]^T$  denote the column vector of unknown channel coefficients between the  $u$ th user and BS and define the row vector

$$\boldsymbol{\lambda}_{i,t}^u(\mu_u) = [\lambda_{i,t}^u(0, \mu_u) \ \dots \ \lambda_{i,t}^u(Q-1, \mu_u)] \quad (15)$$

As a result, (10) can be written as

$$z_i^u[t] = \boldsymbol{\lambda}_{i,t}^u(\mu_u) \mathbf{h}_u + v_i^u[t] \quad (16)$$

In order to express the set of equations (16) in compact vector form, we first introduce:

$$\mathbf{z}_i^u = [z_i^u[t_0] \ z_i^u[t_1] \ \dots \ z_i^u[t_{T_u-1}]]^T \quad (17)$$

$$\boldsymbol{\lambda}_i^u(\mu_u) = [\boldsymbol{\lambda}_{i,t_0}^u(\mu_u)^T \ \boldsymbol{\lambda}_{i,t_1}^u(\mu_u)^T \ \dots \ \boldsymbol{\lambda}_{i,t_{T_u-1}}^u(\mu_u)^T]^T \quad (18)$$

$$\mathbf{v}_i^u = [v_i^u[t_0] \ v_i^u[t_1] \ \dots \ v_i^u[t_{T_u-1}]]^T \quad (19)$$

Therefore, we can write

$$\mathbf{z}_i^u = \boldsymbol{\lambda}_i^u(\mu_u) \mathbf{h}_u + \mathbf{v}_i^u \quad (20)$$

We then stack these vectors and matrices over the frequency index, and define

$$\mathbf{Z}^u = [(\mathbf{z}_1^u)^T \ (\mathbf{z}_2^u)^T \ \dots \ (\mathbf{z}_{|\mathcal{S}_u|}^u)^T]^T \quad (21)$$

$$\boldsymbol{\Lambda}^u(\mu_u) = [\boldsymbol{\lambda}_1^u(\mu_u)^T \ \boldsymbol{\lambda}_2^u(\mu_u)^T \ \dots \ \boldsymbol{\lambda}_{|\mathcal{S}_u|}^u(\mu_u)^T]^T \quad (22)$$

$$\mathbf{V}^u = [(\mathbf{v}_1^u)^T \ (\mathbf{v}_2^u)^T \ \dots \ (\mathbf{v}_{|\mathcal{S}_u|}^u)^T]^T \quad (23)$$

From (20), it then follows that

$$\mathbf{Z}^u = \boldsymbol{\Lambda}^u(\mu_u) \mathbf{h}_u + \mathbf{V}^u \quad (24)$$

where  $\boldsymbol{\Lambda}^u(\mu_u)$  is a  $N_u \times Q$  matrix, assumed to be of full column rank.

As a consequence of the AWGN model assumption, it follows that  $\mathbf{V}^u$  is a complex circular Gaussian random vector with zero-mean and diagonal covariance matrix  $\mathbf{C}_{\mathbf{V}^u} = E[\mathbf{V}^u (\mathbf{V}^u)^H] = \sigma_v^2 \mathbf{I}$ . Accordingly, for given values of the unknown parameters  $\mu_u$  and  $\mathbf{h}_u$ , the observation vector  $\mathbf{Z}^u$  in (24) is also Gaussian with mean  $\boldsymbol{\Lambda}^u(\mu_u) \mathbf{h}_u$  and covariance  $\mathbf{C}_{\mathbf{Z}^u} = \sigma_v^2 \mathbf{I}$ . The probability density function (PDF) of  $\mathbf{Z}^u$ , say  $f(\mathbf{Z}^u; \mu_u, \mathbf{h}_u)$  can therefore be formulated as

$$f(\mathbf{Z}^u; \mu_u, \mathbf{h}_u) = \frac{1}{\pi^{N_u} \det(\mathbf{C}_{\mathbf{Z}^u})} \times \exp[-(\mathbf{Z}^u - \boldsymbol{\Lambda}^u(\mu_u) \mathbf{h}_u)^H \mathbf{C}_{\mathbf{Z}^u}^{-1} (\mathbf{Z}^u - \boldsymbol{\Lambda}^u(\mu_u) \mathbf{h}_u)] \quad (25)$$

Taking the natural logarithm of this PDF, the log-likelihood function (LLF) [13] for the parameters  $\mu_u$  and  $\mathbf{h}_u$  can be expressed (up to a constant term) in the form

$$\mathcal{L}(\mathbf{Z}^u; \mu_u, \mathbf{h}_u) = -\frac{1}{\sigma_v^2} [\mathbf{Z}^u - \boldsymbol{\Lambda}^u(\mu_u) \mathbf{h}_u]^H [\mathbf{Z}^u - \boldsymbol{\Lambda}^u(\mu_u) \mathbf{h}_u] \quad (26)$$

The joint ML estimators of CFO and CIR is obtained by maximizing the LLF (26) with respect to the unknown parameters  $\mu_u$  and  $\mathbf{h}_u$ . Since the LLF is quadratic in the CIR parameters, a closed-form solution can be obtained for the optimum  $\mathbf{h}_u$  in terms of  $\mu_u$  as

$$\mathbf{h}_u^o(\mu_u) = \boldsymbol{\Lambda}^u(\mu_u)^\dagger \mathbf{Z}^u \quad (27)$$

where  $\boldsymbol{\Lambda}^u(\mu_u)^\dagger = (\boldsymbol{\Lambda}^u(\mu_u)^H \boldsymbol{\Lambda}^u(\mu_u))^{-1} \boldsymbol{\Lambda}^u(\mu_u)^H$  is the pseudo-inverse of  $\boldsymbol{\Lambda}^u(\mu_u)$ , which can be pre-computed for a given range of CFO values. Next, upon substitution of (27) into (26), the ML estimate of  $\mu_u$  can be obtained via a 1-dimensional search as

$$\hat{\mu}_u = \arg \max_{\mu_u \in \mathcal{M}_u} \{\mathcal{L}(\mathbf{Z}^u; \mu_u, \mathbf{h}_u^o(\mu_u))\} \quad (28)$$

where  $\mathcal{M}_u$  is the search range for  $\mu_u$ . The first step in the maximization of (28) is the coarse search where  $\mathcal{L}(\mathbf{Z}^u; \mu_u, \mathbf{h}_u^o(\mu_u))$  is computed over a uniform grid of  $\mu_u$  values and the location of its maximum on the grid, say  $\mu_u^m$ , is determined. The second step, or fine search, attempts to find the local maximum nearest to  $\mu_u^m$ , which can be handled by classic optimization methods due to the observed convexity of  $\mathcal{L}(\mathbf{Z}^u; \mu_u, \mathbf{h}_u^o(\mu_u))$  in the vicinity of the true CFO. Then, the ML estimate of the CIR is obtained by substituting  $\hat{\mu}_u$  in (27), that is:

$$\hat{\mathbf{h}}_u = \mathbf{h}_u^o(\hat{\mu}_u) = \boldsymbol{\Lambda}^u(\hat{\mu}_u)^\dagger \mathbf{Z}^u \quad (29)$$

Finally, the single-tap per subband equalizer coefficients, denoted as  $e_i$  for  $i \in \mathcal{S}_u$ , are obtained from the estimated CIR coefficients via the following expression

$$e_i = \frac{1}{\hat{H}_u(z)} \Big|_{z=w^i} \quad (30)$$

where  $\hat{H}_u(z) = \sum_{l=0}^{Q-1} \hat{h}_u[l] z^{-l}$ . Note that except for  $Q$ , no *a priori* information is required to implement the above estimator. Finally, since the subband allocation scheme is known to the receiver, the CFO and CIR of each user can be independently estimated in this way.

To improve the performance of the estimation, the CFO can be estimated iteratively in two steps. The first step is to estimate the CFO as in (28), where  $\hat{\mu}_u^{(1)}$  denotes the resulting value. The second step starts by using  $\hat{\mu}_u^{(1)}$  at the receiver front-end to compensate the CFO for each user, as in

$$\hat{y}_u^{(1)}[m] = \bar{y}[m]e^{-j2\pi\frac{\hat{\mu}_u^{(1)}}{M}m} \quad (31)$$

This CFO compensated signal  $\hat{y}_u^{(1)}[m]$  is then fed into the receiver where the same estimation process is applied again and a second CFO estimate, denoted  $\hat{\mu}_u^{(2)}$ , is obtained through (28). Finally, the CIR and equalizer coefficients are derived based on the refined CFO  $\hat{\mu}_u^{(2)}$  via (29) and (30). The motivation behind this approach is that the interference terms (in particular, the data-interference term  $w_i^u[t]$  in (12)) are smaller when the CFO is nearly compensated and the final estimation accuracy will therefore be improved. Note that in this setup, only two iterations of CFO estimation are considered, whereas more iterations are possible in practice.

#### IV. RESULTS

In this section, we investigate the performance of the proposed joint ML estimator of the CFO and equalizer coefficients in (28)-(30) through numerical simulations. We consider an MU-OPRFB system (cf. Fig. 1) with  $U = 4$  time-synchronized users (results are presented for user  $u = 1$ ), burst size  $N = 60$  symbols,  $M = 64$  subbands,  $K = 72$  up/down-sampling factor, sampling rate  $F_s = 41.67\text{kHz}$ , carrier frequency  $F_c = 800\text{MHz}$  and prototype filter of length  $D = 1728$  designed as in [6]. Each user is allocated 16 subbands based on the schemes illustrated in Fig. 2. The input data sequences  $x_i^u[n]$  consist of independent and equiprobable 4-QAM symbols with unit power, i.e.  $|x_i^u[n]| = 1$ . Without loss in generality, we set  $p_i^u[t] = 1$  for all pairs  $(i, t)$ .

The data at the output of each user's transmitter is passed through a (different) frequency selective wireless channel with randomly generated coefficients  $h_u[l]$ , based on the ITU Vehicular-A channel models [14]. Each channel consists of 8 taps, where the fifth and seventh taps are set to zero and the other taps, with delays 0, 0.33, 0.66, 1, 1.66, 2.33  $\mu\text{s}$ , obey a Rayleigh distribution with relative average powers of 0, -1, -9, -10, -15, -20 dB, respectively. Here, we consider two different channel models, i.e.: time-invariant and time-varying. In the first case, the channel remains constant over the duration of a transmission burst while in the second case, it changes every 0.33  $\mu\text{s}$  according to Jakes's statistical model [15] as a function of the maximum Doppler frequency  $F_d = \frac{vF_c}{c_0}$ , where  $v$  is the mobile speed in m/s and  $c_0 = 3 \times 10^8\text{m/s}$ . At the channel outputs, AWGN with a power level of  $\sigma_v^2$  is added to the baseband received signal to obtain the desired SNR figure, defined as  $\text{SNR} = \sigma_s^2 / \sigma_v^2$  with  $\sigma_s^2 = E\{|y_u[m]|^2\}$ . For each choice of parameter set, we run  $10^3$  independent Monte Carlo trials and compute the relevant performance measures under evaluation, i.e., the root mean squared error (RMSE) of the CFO and equalizer coefficients estimates.

The RMSE performance of the proposed joint estimator of the CFO and equalizer coefficients as a function of SNR is presented in Fig. 4 for the various subband allocation schemes,

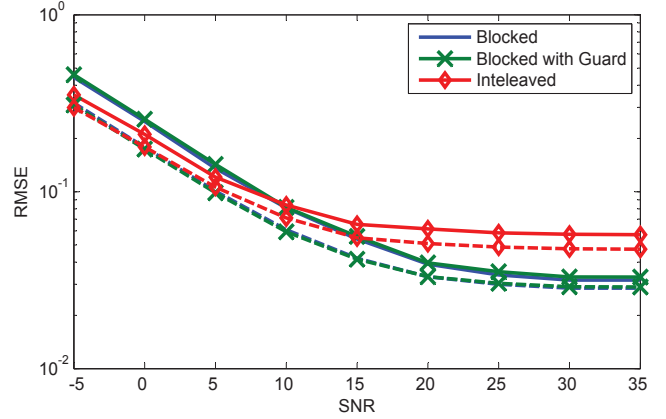


Fig. 4. RMSE of CFO (solid lines) and Equalizer (dashed lines) estimation versus SNR ( $\mu_u = 5\%$ ,  $T_u = 6$  and  $G = 1$ )

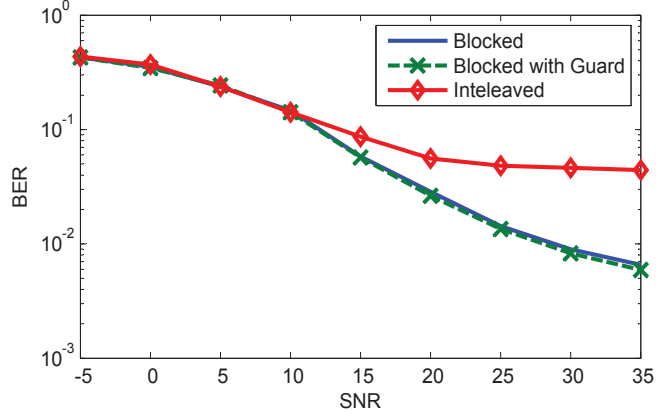


Fig. 5. BER versus SNR ( $\mu_u = 5\%$ ,  $T_u = 6$  and  $G = 1$ )

where the following parameter values are used: true CFO  $\mu_u = 5\%$ ,  $T_u = 6$  and  $G = 1$ . It can be seen that the estimation performance is very similar for the blocked and blocked with guard allocation schemes. Therefore, considering the fact that some subbands are not utilized in the latter scheme, it is preferable to employ the block scheme. At mid to high SNR, the interleaved scheme generally exhibits the largest estimation error among the allocation schemes. Keeping the same settings, the uncoded BER performance of the OPRFB transceiver with CFO compensation and equalization using the estimated parameters is plotted in Fig. 5. Similar to the RMSE results, the proposed method shows a superior performance for the blocked schemes (with or without guard).

The RMSE performance of the proposed CFO and equalizer coefficients estimators using the iterative method is depicted in Fig. 6, where the same parameters as in Fig. 4 are used. Comparing the two figures, it can be seen that in general, the performance of the joint estimator considerably improves when using the iterative method. In particular, and in contrast to the non-iterative method, the iterative one performs equally well for all the considered allocation schemes. Similarly, the BER performance of the proposed CFO compensation and equalization method using iteratively estimated parameters is plotted in Fig. 7. As expected, compared to Fig. 5, the BER of the system employing iterative estimation is greatly improved.

Next, we investigate the performance of the proposed joint ML estimator under time-varying channel conditions for the

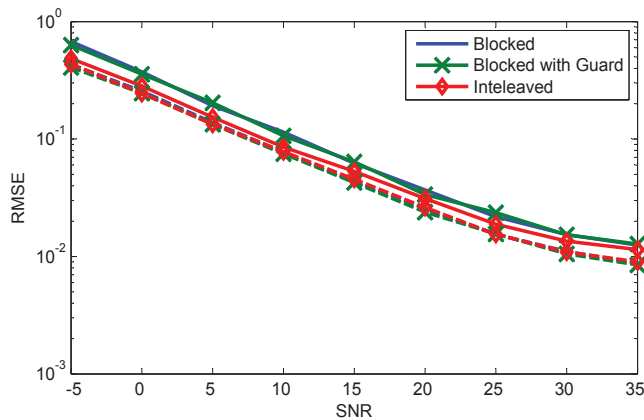


Fig. 6. RMSE of CFO (solid lines) and Equalizer (dashed lines) iterative estimation versus SNR ( $\mu_u = 5\%$ ,  $T_u = 6$  and  $G = 1$ )

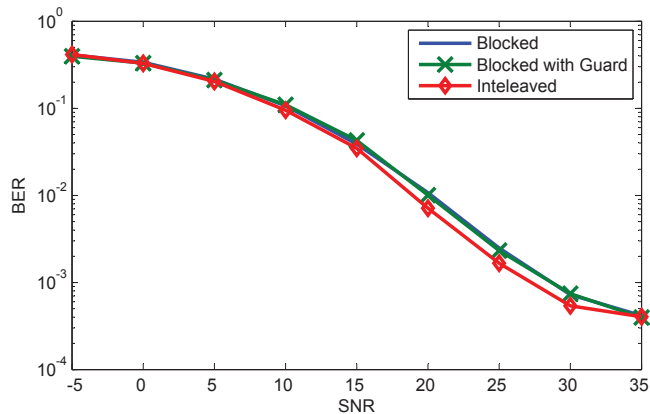


Fig. 7. BER versus SNR ( $\mu_u = 5\%$ ,  $T_u = 6$  and  $G = 1$ ) with iterative estimation

blocked subband allocation scheme. In Fig. 8, the RMSE performance of the CFO and equalizer coefficient estimators (iterative scheme) is plotted as a function of the maximum Doppler frequency  $F_d$  for various temporal distributions of pilots, where the following parameter values are used:  $\mu_u = 5\%$ ,  $T_u = 12$  and  $\text{SNR}=30\text{dB}$ . In particular, pilots are divided into  $G = 1, 2$  and  $3$  groups and  $G$  different estimators of equalizer's coefficients corresponding to each group of pilots are obtained, whereas the CFO is assumed to remain fixed over time. The values of  $F_d$  in Fig. 8, are equivalent to 4 different mobile speeds, that is 5, 60, 120 and 250 km/h corresponding to pedestrian, car in urban area, car on the highway and high-speed train, respectively. The comparisons between these patterns show that for low mobility, the desired parameters can be better estimated by the preamble implementation of the pilots, i.e.,  $G = 1$ . However, with increased mobility, the scattered pilot schemes, i.e.,  $G = 2$  or  $3$ , offer a slightly better performance in estimation.

## V. CONCLUSION

In this paper, we considered the problem of joint data-aided CFO and equalizer coefficients estimation in the uplink of MU-OPRFB systems. By exploiting statistical properties of inserted pilots transmitted by such systems over a frequency selective channel, the ML estimator for the unknown parameters was derived. This method was tested over frequency

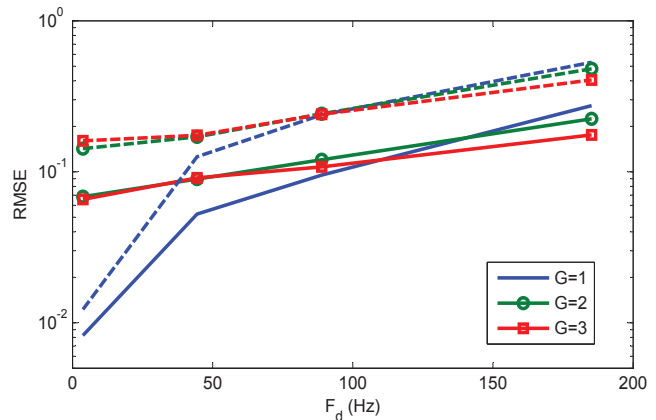


Fig. 8. RMSE of CFO (solid lines) and Equalizer (dashed lines) iterative estimation versus Doppler frequency ( $\mu_u = 5\%$ ,  $T_u = 12$  and  $\text{SNR}=30\text{dB}$ )

selective channel with different subband allocation schemes. Moreover, different pilot patterns were considered for the proposed estimation method over time-varying channels. The simulation results demonstrate that over a wide range of experimental conditions, the proposed joint ML estimator (along with associated CFO compensation and equalization mechanisms) provides a reliable performance in uplink MU-OPRFB transmissions.

## REFERENCES

- [1] A. Larimo, M. Lindstrom, M. Meyer, G. Pelletier, J. Torsner, and H. Wiermann, "The LTE link-layer design," *IEEE Commun. Mag.*, vol. 47, pp. 52–59, April 2009.
- [2] M. Morelli, C.-C. Kuo, and M.-O. Pun, "Synchronization techniques for orthogonal frequency division multiple access (OFDMA): A tutorial review," *Proceedings of the IEEE*, vol. 95, pp. 1394–1427, July 2007.
- [3] B. Farhang-Boroujeny, "OFDM versus filter bank multicarrier," *IEEE Signal Process. Mag.*, vol. 28, pp. 92–112, May 2011.
- [4] H. Saeedi-Sourck, Y. Wu, J. Bergmans, S. Sadri, and B. Farhang-Boroujeny, "Complexity and performance comparison of filter bank multicarrier and OFDM in uplink of multicarrier multiple access networks," *IEEE Trans. Signal Process.*, vol. 59, pp. 1907–1912, April 2011.
- [5] T. Fusco, A. Petrella, and M. Tanda, "Sensitivity of multi-user filter-bank multicarrier systems to synchronization errors," in *Proc. Int. Symp. Commun., Control, Signal Process.*, March 2008, pp. 393–398, St. Julians, Malta.
- [6] S. Rahimi and B. Champagne, "Oversampled perfect reconstruction DFT modulated filter banks for multi-carrier transceiver systems," *Signal Process.*, vol. 93, pp. 2942–2955, Nov. 2013.
- [7] D. Pinchon and P. Siohan, "Oversampled paraunitary DFT filter banks: A general construction algorithm and some specific solutions," *IEEE Trans. Signal Process.*, vol. 59, no. 7, pp. 3058–3070, July 2011.
- [8] S. Rahimi and B. Champagne, "Carrier frequency recovery for oversampled perfect reconstruction filter bank transceivers," in *Proc. Int. Conf. Wireless Mobile Commun.*, Nice, France, July 2013, pp. 140–145.
- [9] V. Lottici, R. Reggiannini, and M. Carta, "Pilot-aided carrier frequency estimation for filter-bank multicarrier wireless communications on doubly-selective channels," *IEEE Trans. Signal Process.*, vol. 58, pp. 2783–2794, May 2010.
- [10] D. Mattered and M. Tanda, "Data-aided synchronization for OFDM/OQAM systems," *Signal Process.*, vol. 92, pp. 2284–2292, Sep. 2012.
- [11] S. Rahimi and B. Champagne, "Joint channel and frequency offset estimation for oversampled perfect reconstruction filter bank transceivers," *IEEE Trans. Commun.*, vol. 62, pp. 2072–2084, 2014.
- [12] J. A. Rice, *Mathematical Statistics and Data Analysis*, 2nd ed. Stamford, CT, USA: Cengage Learning, 2007.
- [13] S. Kay, *Fundamentals of Statistical Signal Processing, Vol. I: Estimation Theory*. Upper Saddle River, NJ, USA: Prentice Hall, 2001.
- [14] Recommendation ITU-R M. 1225. (1997) Guidelines for evaluation of radio transmission technologies for IMT-2000.
- [15] W. Jakes, *Microwave Mobile Communications*. Piscataway, NJ, USA: Wiley-IEEE Press, 1994.